Numerical parametric study of geofoam seismic buffers with different constitutive models

Zarnani, S.
Graduate student, GeoEngineering Centre at Queen's-RMC, Department of Civil Engineering, Queen's University, Kingston, Ontario, K7L 3N6

Bathurst, R.J.
Professor, GeoEngineering Centre at Queen's-RMC, Department of Civil Engineering, Royal Military College of Canada, Kingston, Ontario, K7K 7B4, Phone: (613) 541-6000 (ext. 6479/6347/6391); FAX: (613) 545-8336, Email: bathurst-r@rmc.ca

Keywords: geofoam, seismic buffer, constitutive model, numerical parametric study

ABSTRACT: Experimental tests and numerical simulations have shown that a vertical inclusion of EPS geofoam material placed against a rigid soil retaining wall can reduce both static and dynamic loads acting on the wall before and during earthquake. In the current numerical parametric study a rigid retaining wall with fixed height of 6 m was considered with different EPS materials. Also investigated was the influence of the constitutive model for EPS geofoam on numerical outcomes. The constitutive models considered were as follows: a) simple elasto-plastic model with constant Rayleigh damping, b) advanced non-linear model with variable hysteresis damping (equivalent linear model, ELM) and, c) strain-hardening model. A FLAC model that has been verified against reduced-scale shaking table tests was used to run the simulations. The results show that for the parameters investigated in this study, there is not a significant variation in load attenuation acting on the wall for models with different EPS constitutive models but choice of model may have an important influence on the magnitude of buffer compression and hence affect the serviceability of the wall and the performance of structures in close proximity to the wall. The variation in isolation efficiency is only a few percentage points for the EPS constitutive models used but in general the simulation with hardening model for EPS showed smaller buffer compression.

1 INTRODUCTION

The concept of earth pressure reduction for rigid retaining walls under static and dynamic loading conditions has been investigated both experimentally and numerically by a number of researchers. Earth pressure reduction can be achieved by introducing a suitable layer of compressible material between the rigid wall and the backfill material. This inclusion can reduce earth pressures to levels close to the active state (minimum theoretical value) for static loading conditions. The material of choice is expanded polystyrene (EPS) which is called geofoam in the geotechnical literature and is available with a range of densities and compressive properties.

Karpurapu and Bathurst (1992) used a verified finite element method (FEM) numerical model to develop a series of design charts that can be used to select the properties of the compressible layer for static loading conditions.

Shaking table experiments on 1-m high rigid retaining wall models were carried out at the Royal Military College of Canada (RMC) (Bathurst et al. 2007; Zarnani and Bathurst 2007). They demonstrated that the compressible inclusion concept can be extended to reduce large earthquake-induced loads against rigid retaining walls. A compressible layer for dynamic load attenuation is called a seismic buffer. Numerical simulations are also a powerful tool to quantitatively investigate the benefit of seismic buffers in rigid retaining wall applications. Zarnani and Bathurst (2008) first developed a finite difference method (FDM) numerical model. Their numerical model was verified against the RMC experimental results and it was shown that the simulation results were qualitatively and in most cases quantitatively in good agreement with measured experimental values. The same numerical approach was then used to investigate the influence of two different constitutive models for the soil and seismic buffer on the accuracy of RMC shaking table test simulations (Zarnani and Bathurst 2009a). Their numerical simulation results demonstrated that the more advanced equivalent linear method (ELM) constitutive model did not significantly improve simulation accuracy com-

pared to the simpler elastic-perfectly plastic constitutive model with Mohr-Coulomb failure criterion (MC). The effect of other parameters such as seismic buffer thickness, stiffness, wall height and base excitation characteristics were investigated in a numerical parametric study by Zarnani and Bathurst (2009b) using the MC model for buffer and soil materials.

The work reported in this paper, is a continuation of numerical modeling of seismic buffers by the writers. In this paper a typical rigid wall of height H = 6 m is selected together with a constant seismic buffer thickness t = 0.9 m. Three different constitutive models of varying complexity were used to simulate the behavior of the seismic buffers in numerical simulations. The numerical models were excited at the base and far-field boundary using a synthetic earthquake record developed for western Canada. This input accelerogram was modified to investigate the influence of proximity of the predominant frequency of the record to the natural frequency of the wall system.

2 NUMERICAL MODEL

The finite difference numerical program FLACv5 (Itasca 2005) was used for this numerical analysis. Figure 1 shows the cross section of the numerical grid used in the current study. The model height (H) was fixed at 6 m and the width of the retained soil (B) kept constant at 30 m; hence, the model aspect ratio B/H = 5. This ratio was selected based on previous similar numerical simulations carried out by Bathurst and Hatami (1998) and Zarnani and Bathurst (2009b). The thickness of seismic buffer (t) was fixed at 0.9 m which is equivalent to 15% of the wall height (t/H = 0.15). The grid density (zone size = 0.3 m) was selected based on previous sensitivity analysis (Zarnani and Bathurst 2009b).

The vertical sides and bottom of the numerical domain had fixed velocity boundaries in both X and Y directions. During the dynamic loading stage, the prescribed acceleration record was applied to these three boundaries. The rigid wall was 0.6 m thick and had stiffness 1000 times greater than the backfill soil. Free vibration analysis of the numerical model revealed that the fundamental frequency of the model (f_{11}) is about 2.8 Hz. Interface layers were introduced between the rigid wall and EPS layer and between the EPS layer and the backfill material. These zero thickness interface layers allowed slip and separation to occur between material zones. The interface between the rigid wall and EPS layer had a friction angle of 25 degrees and the interface friction angle between the EPS layer and the backfill soil was 20 degrees. These values were based on back-calculation from experimental shaking table test results reported by Zarnani and Bathurst (2007).

3 MATERIAL PROPERTIES

In order to limit the number of variables, the soil properties were kept constant in all simulations. The soil was modeled as elastic-perfectly plastic material with Mohr-Coulomb failure criterion with a very low cohesion value (3 kPa). This small cohesion was used in all models to ensure numerical stability at the unconfined soil surface when models were excited at high frequencies. Five percent Rayleigh damping was also applied to the soil domain in all simulations. The equations of motion in matrix form include a damping matrix which is used to damp the natural oscillation modes of the system. This damping matrix for linear elastic equations of motion, which has components proportional to mass and stiffness of the system, is known as Rayleigh damping in dynamic analysis. The properties of the backfill material are presented in Table 1. These properties are considered typical of loose to medium dense sand.

Table 1. Backfill properties

Property	Value
Unit weight (kN/m^3)	17.2
Friction angle (degrees)	35
Cohesion (kPa)	3
Dilation angle (degrees)	10
Shear modulus (MPa)	16
Bulk modulus (MPa)	21
Shear wave velocity (m/s)	96

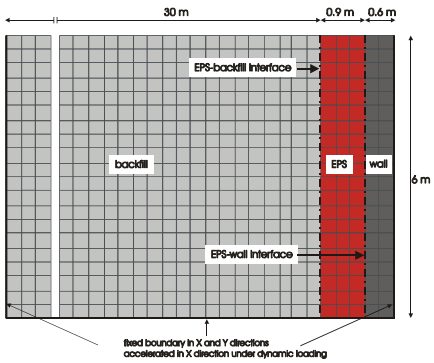

Figure 1. FLAC numerical grid

Two different EPS materials were used in the current numerical parametric study. Based on ASTM D-6817 standard (ASTM 2006) EPS materials are

classified according to density. In this study EPS15 and EPS29 with minimum densities of 14.4 and 28.8 kg/m^3 were used. Previous experimental studies plus the results of compression tests by the writers presented later have shown that EPS material behaves as linear elastic material up to compressive strains of about 1%. However, after yield EPS material undergoes a hardening stage during which the strength of EPS increases as strain increases. Hardening behavior of EPS has been studied by some researchers. Wong and Leo (2006) proposed a simple elasto-plastic hardening model for EPS geofoam for strain levels below the sigmoidal strain (i.e. before rapid strain hardening occurs). Their model requires six independent parameters that can be deduced from triaxial tests. Hazarika (2006) proposed a constitutive model for EPS for large strain applications based on the incremental theory of plasticity. The material parameters of the constitutive model were determined from a series of unconfined compression tests and included different EPS specimen shapes, sizes and densities. A hyperbolic constitutive model was also proposed for EPS as a function of density and confining stress by Chun et al. (2004).

The choice of constitutive model adopted for EPS material may be expected to have an important influence on the results of numerical simulations. Three different models were used in the current investigation: (1) linear-elastic purely cohesive material with Mohr-Coulomb failure criterion and constant Rayleigh damping (MC); (2) equivalent-linear method with variable hysteresis damping and Mohr-Coulomb failure criterion (ELM+MC), and; (3) strain hardening model with Mohr-Coulomb failure criterion (HARD+MC).

Figure 2 illustrates unconfined compression test results on 250 mm cube specimens of EPS15 and EPS29 that were carried out by the writers. These results clearly show the linear elastic range, the yield point and the subsequent hardening stage. For the MC model, the EPS behaves linearly elastic up to the compression yield point (defined as twice the cohesive strength) at which point the material undergoes plastic deformation with constant load capacity; hence, hardening behavior cannot be captured. However, MC model approximations for two different EPS materials are fitted to the data as illustrated in Figure 2. Despite the limitations of this simple model, it has proved sufficiently accurate in previous numerical simulations of the RMC shaking table tests (Zarnani and Bathurst 2008). For dynamic simulations, a constant Rayleigh damping of 5% was applied to the EPS zone.

The second EPS constitutive model (ELM+MC) is based on the concept of shear modulus reduction and increase of hysteresis damping with increasing shear strain. Shear modulus degradation and increase in hysteresis damping is the result of hysteresis stress-strain loops with progressively shallower slopes and greater width as shear strain increases. Details of the adaptation of this constitutive model for EPS materials in FLAC numerical simulations have been reported by Zarnani and Bathurst (2009a). Figure 3 illustrates the shear modulus reduction and damping ratio changes with shear strain for different EPS materials. In some previous studies it was shown that the density of EPS material and the magnitude of confining pressure do not have a significant effect on the shear modulus degradation curve (Athanasopoulos et al. 1999, 2007; Ossa and Romo 2008). Also shown in Figure 3 are the results of resonant column tests on EPS15 and EPS29 at 0 and 20 kPa confining pressure carried out by the writers. The resonant column results by the writers show slightly stiffer behavior compared to earlier investigations. The degradation curve that was adopted for the ELM model in the current numerical study was selected to fall between data reported by others and more recent data by the writers. Degradation curves for the equivalent-linear elastic method (ELM) were used along with the same shear yield strength (cohesion) for the geofoam (i.e. Mohr–Coulomb failure criterion). In this model, EPS cyclic response remains continuously non-linear below the yield strength.

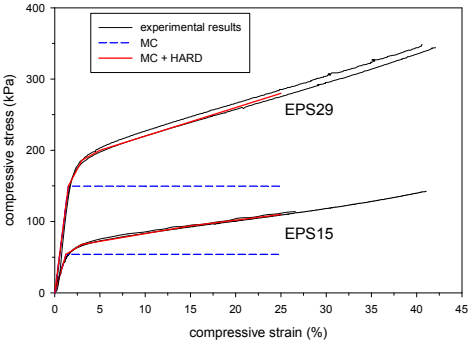

Figure 2. Compressive stress-strain behavior of EPS

The third EPS constitutive model (HARD+MC) is based on the Mohr-Coulomb failure criterion but with the possibility of strength parameter hardening after the onset of plastic yield. In the hardening model in FLAC (Itasca 2005) the user can define strength parameters as piece-wise linear functions of the hardening parameter which in turn is a function of plastic shear strain. The code records the total plastic shear strain by incrementing the hardening parameters at each time step and adjusts model properties to conform to the user-defined functions

(Itasca 2005). In the current investigation the cohesive shear strength parameter of the EPS material was changed with plastic shear strain as illustrated in Figure 2. It is clear that this hardening model is better able to capture EPS behavior at higher strain levels than the MC model. A constant Rayleigh damping ratio of 5% was also used for simulations using this constitutive model.

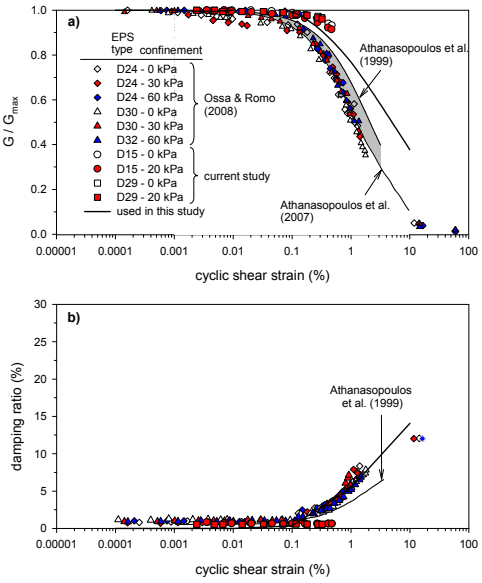

Figure 3. Shear modulus and damping variation of EPS material with shear strain

The shear strength parameters used for two different types of EPS are presented in Table 2. These material properties were based on experiments performed by the writer and correlations available in the literature.

Table 2. EPS properties

Property	Type	
	EPS15	EPS29
Density (kg/m^3)	15	29
Yield (compressive) strength (kPa)	54	150
Cohesion (shear strength) (kPa)	27	75
Shear modulus (MPa)	2	4.5
Bulk modulus (MPa)	1.7	4.13

4 MODEL EXCITATION

In this study, one of a series of synthetic earthquake records developed for western Canada by Atkinson and Beresnev (1998) was used as the excitation record applied to the numerical model. This record (Figure 4) identified as M6.5, R30 (M = moment magnitude of earthquake, R = distance of the earthquake from the city in km) is a short period event for cities of Vancouver and Victoria in British Columbia. The magnitude of the acceleration was scaled to 0.6g (PA=peak acceleration) for this numerical study. The fast Fourier transform (FFT) analysis of this record shows that it has a predominant frequency (f) of about 1.3 Hz. In order to investigate the effect of predominant frequency of the earthquake record on the results, the time increment of the original record was adjusted to achieve predominant frequencies of 0.6 Hz, 2.99 Hz and 3.37 Hz. It has been shown that the proximity of the fundamental frequency of excitation to the natural frequency of the structure has a very significant impact on the seismic performance of these structures (Zarnani and Bathurst 2009b). Based on the 2.8 Hz natural frequency of the model (f_{11}), different frequency proximity ratios (f/f_{11}) were investigated. Table 3 summarizes different characteristics of the excitation records.

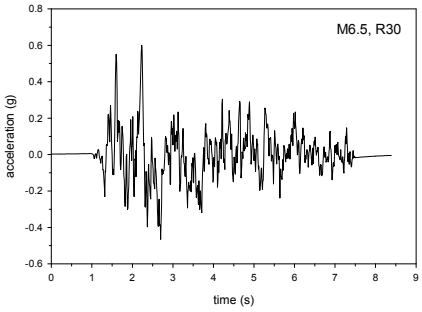

Figure 4. The acceleration record (M6.5, R30)

5 NUMERICAL RESULTS AND DISCUSSION

The most important function of EPS seismic buffers is dynamic load attenuation. Hence, wall force results are the focus of this current investigation. Figure 5 shows the temporal variation of total wall force acting on the rigid retaining wall using the MC+HARD model for EPS.

The maximum calculated wall force for the case of no EPS seismic buffer was compared to the maximum wall force with an EPS seismic buffer. An isolation efficiency factor was defined to quantify the relative performance of the EPS wall with respect to load attenuation (Zarnani and Bathurst 2009b). This parameter is computed as the difference in total measured wall force with and without a seismic buffer (force attenuation) divided by the wall force for the control case (without buffer) in percent. Figure 6a and 6b show, respectively, the

maximum wall force calculated during model excitation and the isolation efficiency for different numerical simulations with different EPS material types and different EPS constitutive models. In all cases, the maximum wall force is much less using a layer of EPS seismic buffer placed against the rigid retaining wall. The amount of wall force reduction is higher for the models with the more compressible EPS15 buffers compared to the models with EPS29. Figure 6a also illustrates that the magnitude of maximum wall force for the models with EPS seismic buffer is not significantly affected by the choice of EPS constitutive model. Figure 6b shows that for the parameters investigated in this study, there is not a significant variation in isolation efficiency for models with different EPS constitutive models. The variation in isolation efficiency is only a few percentage points for the EPS constitutive models used.

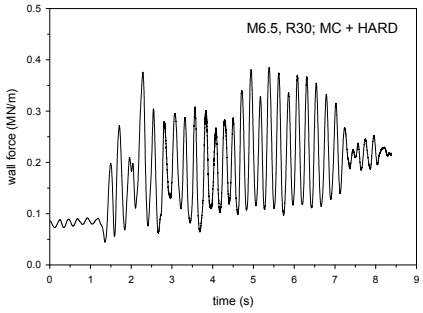

Figure 5. Typical total wall force response with time

Table 3. Excitation record characteristics

Excitation record	property		
	PA (g)	f (Hz)	f/f_{11}
M6.5, R30_f0.6	0.6	0.6	21%
M6.5, R30	0.6	1.3	46%
M6.5, R30_f3	0.6	3	107%
M6.5, R30_f3.37	0.6	3.37	120%

Another performance feature of interest is the compression of the EPS buffer during excitation. Profiles of time-coincident maximum EPS buffer compression along the height of the rigid wall are presented in Figure 7 for all numerical simulations. It can be seen that the maximum buffer compression is significantly higher for EPS15 compared to EPS29. This is attributed to the more compressible behavior of the lower density EPS material. Also, when results of maximum buffer compression of EPS15 are compared it can be seen that in most cases the maximum buffer compression occurs for simulations with MC constitutive model for EPS buffers and the smallest buffer compression generally occurs when the MC+HARD constitutive model for EPS is used. For example, Figure 7b shows the greatest buffer compression for EPS15 (excited with original M6.5, R30 record at 46% of f_{11}). The maximum buffer compression from all simulations is about 5.5% which means that the material should be in the hardening stage (Figure 2). However, using the hardening model (MC+HARD) for the EPS layer the maximum buffer compression is reduced to about 3%.

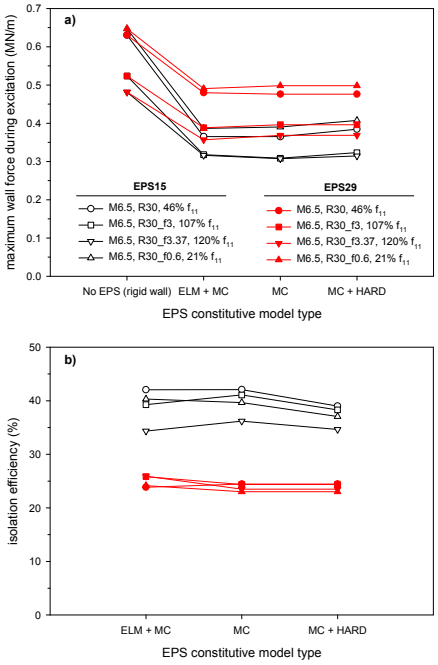

Figure 6. Maximum wall force and isolation efficiency for different models

For the models with EPS29 the effect of EPS constitutive model on buffer compression is not significant because of its higher density and stiffness. For all simulations using EPS29 the maximum buffer compression did not exceed the elastic limit of the material, hence the choice of EPS constitutive model did not have any significant effect on buffer compression at these low strain levels.

The magnitude of buffer compression may influence other performance limit states. If too much compression occurs in the buffer during seismic loading, then excessive deformation of structures located on the backfill surface close to the wall could occur. Hence, for design of a seismic buffer placed against a rigid retaining wall, both load reduction (or isolation efficiency) and ground deformations in proximity to the wall should be considered. In conclusion, the most important findings from this numerical investigation are that for the range of parameters investigated, the choice of constitutive model for EPS seismic buffer may not

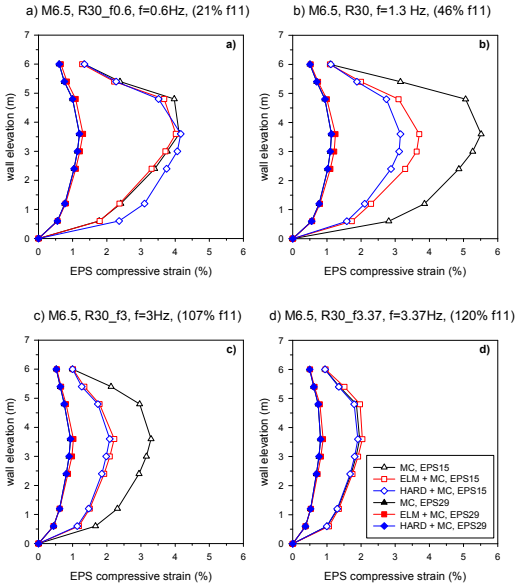

Figure 7. Maximum buffer compression for all models

have a significant effect on load attenuation but it may have an important influence on the magnitude of buffer compression and hence influence the serviceability of the wall and the performance of structures in close proximity to the wall. However, the more complex constitutive models (ELM+MC, HARD+MC) require more parameters to define the material models and more experimental data to back-fit the model parameters. They are also more computationally intensive than the simple linear elastic plastic MC model.

ACKNOWLEDGEMENTS

The authors thank Dr. Giovanni Cascante for allowing them to perform resonant column tests on EPS geofoam at the University of Waterloo and his advice to interpret the test results.

REFERENCES

ASTM D6817-06. 2006. Standard specification for rigid cellular polystyrene geofoam. American Society for Testing and Materials, West Conshohocken, PA, USA.

Athanasopoulos, G.A., Pelekis, P.C. and Xenaki, V.C. 1999. Dynamic properties of EPS geofoam: An experimental investigation. Geosynthetics International, 6(3): 171-194.

Athanasopoulos, G.A., Nikolopoulou, C.P., Xenaki, V.C. and Stathopoulou, V.D. 2007. Reducing the seismic earth pressure on retaining walls by EPS geofoam buffers–numerical parametric study, In CD Proceedings of 2007 Geosynthetics Conference, Washington, D.C., 15 p.

Atkinson, G.M. and Beresnev, I.A. 1998. Compatible ground-motion time histories for new national seismic hazard maps. Canadian Journal of Civil Engineering, 25: 305-318.

Bathurst, R.J. and Hatami, K. 1998. Seismic response analysis of a geosynthetic reinforced soil retaining wall. Geosynthetics International, 5(1&2): 127-166.

Bathurst, R.J., Zarnani, S. and Gaskin, A. 2007. Shaking table testing of geofoam seismic buffers. Soil Dynamics and Earthquake Engineering, 27(4): 324-332.

Chun, B.S., Lim, H.S., Sagong, M. and Kim, K. 2004. Development of a hyperbolic constitutive model for expanded polystyrene (EPS) geofoam under triaxial compression tests. Geotextiles and Geomembranes, 22(4): 223-237.

Hazarika, H. 2006. Stress–strain modeling of EPS geofoam for large-strain applications. Geotextiles and Geomembranes, 24(2): 79-90.

Itasca Consulting Group. 2005. FLAC: Fast Lagrangian Analysis of Continua, version 5. Itasca Consulting Group, Inc., Minneapolis, MN.

Karpurapu, R. and Bathurst, R.J. 1992. Numerical investigation of controlled yielding of soil-retaining wall structures. Geotextiles and Geomembranes, 11(2): 115-131.

Ossa, A. and Romo, M.P. 2008. A model for EPS dynamic shear modulus and damping ratio. In CD Proceedings of First Pan American Geosynthetics Conference and Exhibition, 2-5 March 2008, Cancun, Mexico, pp. 894-901.

Wong, H. and Leo, C.J. 2006. A simple elastoplastic hardening constitutive model for EPS geofoam. Geotextiles and Geomembranes, 24(5): 299-310.

Zarnani, S. and Bathurst, R.J. 2007. Experimental investigation of EPS geofoam seismic buffers using shaking table tests. Geosynthetics International, 14(3): 165-177.

Zarnani, S. and Bathurst, R.J. 2008. Numerical modeling of EPS seismic buffer shaking table tests. Geotextiles and Geomembranes, 26(5): 371-383.

Zarnani, S. and Bathurst, R.J. 2009a. Influence of constitutive model on numerical simulation of EPS seismic buffer shaking table tests. Geotextiles and Geomembranes, 27(4): 308-312.

Zarnani, S. and Bathurst, R.J. 2009b. Numerical parametric study of EPS geofoam seismic buffers. Canadian Geotechnical Journal, 46(3): 318-338.